Acta Oceanol. Sin., 2022, Vol. 41, No. 1, P. 118–131
https://doi.org/10.1007/s13131-021-1861-8
http://www.aosocean.com
E-mail: ocean2@hyxb.org.cn

Benthic microbial biogeography along the continental shelf shaped by substrates from the Changjiang River plume

Yongjun Wei[1], Shan Jiang[2]*, Lingmin Tian[3], Liping Wei[4]*, Jie Jin[2], Juan Severino Pino Ibánhez[5, 6], Yan Chang[2], Xiaodao Wei[7], Ying Wu[2]

[1] Key Laboratory of Advanced Drug Preparation Technologies of Ministry of Education, School of Pharmaceutical Sciences, Zhengzhou University, Zhengzhou 450001, China

[2] State Key Laboratory of Estuarine and Coastal Research, East China Normal University, Shanghai 200241, China

[3] Department of Food Science and Engineering, Jinan University, Guangzhou 510632, China

[4] Key Laboratory of Vegetation Restoration and Management of Degraded Ecosystems, South China Botanical Garden, Chinese Academy of Sciences, Guangzhou 510650, China

[5] School of Natural Sciences, Trinity College Dublin, Dublin 2, Ireland

[6] Instituto de Investigacións Mariñas, Consejo Superior de Investigaciones Científicas, Vigo 36208, Spain

[7] Institute of Eco-Chongming, East China Normal University, Shanghai 202162, China

Received 8 January 2021; accepted 20 May 2021

Abstract

Coastal zones are active reactors of continental material including that transported by rivers via a series of microbiota-mediated reactions. Nevertheless, current knowledge of the ecology and functioning of the microbiota in coastal areas affected by large riverine inputs remains insufficient on a global scale. Here, an investigation on sediment microbial composition, including taxonomy and metabolic network, as well as their relationship with major benthic reaction substrates, namely carbon, nitrogen, sulphur and phosphorus, was conducted in the continental shelf affected by the spread of the Changjiang River plume. Surface sediment samples (48 samples) were collected during March 2018, obtaining a mean Operational Taxonomic Units (OTUs) number of 3 341. Proteobacteria, Acidobacteria and Actinobacteria were abundant phyla in the studied sediments. Bray-Curtis distance analysis classified the 48 samples into 4 clusters (MG1 to MG4) at the phylum-level. MG1 and MG2 are found near the river mouth, receiving substantial land-derived particles from the Changjiang River runoff. Particle-attached microbes may be settled in these regions and influenced the observed sediment microbial diversity and biomass, e.g., increased Crenarchaeota relative abundance. The relative enrichment of these two groups in heterotrophic microbes further suggests a reliance of benthic microbiota on substrates with terrestrial origin, particularly specialized on processing sulphur-rich substrates. Regions MG3 and MG4 are located in the outer margin of the area affected by the Changjiang River plume, mainly fed by settling pelagic particles from phytoplankton. Compared to MG1 and MG2, a significant increase in the abundance of Thaumarcheota (phylum-level) and *Nitrosopumilus* (genus-level) was found in MG3, suggesting nitrogen-related transformations as the key reactions to sustain microbial metabolism in this region. Coupled with the identified variations in the taxonomic composition, significant differences in the keystone taxa between MG1/MG2 and MG3/MG4 were identified via OTU co-occurrence analyses. A higher abundance of Actinobacteria, Thaumarchaeota and Acidobacteria in MG3 and MG4 reinforced the identified spatial variability in benthic metabolism and highlighted the significance of substrate inputs on the sediment microbial structure and biogeography.

Key words: benthic microbiota, biogeography, benthic substrate, Changjiang River plume, East China Sea, Yellow Sea

Citation: Wei Yongjun, Jiang Shan, Tian Lingmin, Wei Liping, Jin Jie, Ibánhez Juan Severino Pino, Chang Yan, Wei Xiaodao, Wu Ying. 2022. Benthic microbial biogeography along the continental shelf shaped by substrates from the Changjiang River plume. Acta Oceanologica Sinica, 41(1): 118–131, doi: 10.1007/s13131-021-1861-8

1 Introduction

Coastal zones are among the most productive marine ecosystems due to the interaction between continental surface loadings and coastal seawater (Kim et al., 2018). The transport of riverine freshwater into continental shelves introduces significant quantities of land-derived particles and boosts the growth of primary producers via adding nutrients and trace elements (Chang et al., 2020, 2021; Jiang et al., 2021b). The combined effect of large river fluxes, coastal currents and the buoyancy of riverine plume waters caused by density differences can transport this terrestrial material very far from the river mouth, thus dramatically changing the composition of large coastal areas (Fournier et al., 2016;

Foundation item: The National Natural Science Foundation of China under contract Nos 31800079 and 41530960; the Scientific Research Foundation of SKLEC under contract No. 2017RCDW04; the Zhengzhou University Startup Foundation under contract No. 32210876; the China Postdoctoral Science Foundation under contract No. 2021M691018.
*Corresponding author, E-mail: sjiang@sklec.ecnu.edu.cn; weilp@scbg.ac.cn

Ibánhez et al., 2016; Lefèvre et al., 2017). These terrestrial and pelagic materials boom the growth and metabolism activity of different pelagic and benthic microbes in the areas affected.

Current research estimates that coastal sediments host more than 35 000 different species of bacteria and archaea on a global scale (Sunagawa et al., 2015), although the benthic microbial composition of continental shelves has received less attention (Wei et al., 2016). Abundant coastal benthic microbes correspond to the phyla of Proteobacteria, Cyanobacteria and Bacteroidetes, while opportunistic benthic phyla such as Firmicutes, Nitrospirae, and Lentisphaerae are commonly found (Chen et al., 2019; Wei et al., 2016; Yu et al., 2012). The diversity and abundance of these benthic communities might be linked to a wide range of environmental parameters, such as sediment particle size, temperature and salinity. Among these parameters, substrates used in metabolic reactions, including organic carbon (OC), nitrogen (N) and sulfur (S) contents, are frequently deemed to be prominent in shaping the microbial biogeography (Brandsma et al., 2013; Sintes et al., 2013; Kuypers et al., 2018).

Microbes in marine environments include the free-living type that distributes in water parcels and the particle-dependent type that is attached to the suspended material or sediment particles (Smith et al., 2013). Due to the abundant environmental microniches provided by particles (Bertics and Ziebis, 2010), the density of particle-dependent microbes, especially in surface sediments, is usually much higher than that of the free-living microbes (Smith et al., 2013). Microbial communities in sediments are responsible for a wide range of benthic reactions, such as organic matter remineralization (Gudasz et al., 2010), nitrification and denitrification (Jiang et al., 2021a; Wang et al., 2018), and S reduction (Pallud and van Cappellen, 2006). The sediment microbes actively use benthic substrates for their metabolic reactions and in turn, the microbial distribution is deeply influenced by the supply of substrates from the overlying waters.

The Changjiang River, the longest river in China (6 300 km) and also called the Yangtze River, delivers ca. 9×10^{11} m^3/a of freshwater into the East China Sea and the Yellow Sea, and is the 5th largest river in the world (Jiang et al., 2021b). A large river plume develops a significant area outside of the river mouth and transports the Changjiang Diluted Water (CDW) far from the river mouth (Chang et al., 2016; Jiang et al., 2021b). Active biogeochemical reactions in the region influenced by the CDW were observed fueled by terrestrially-derived C, N and S (Jiao et al., 2018; Zhang et al., 2019). Similar to the spatial gradients observed in the water column, sediment properties in the area of influence of the Changjiang River plume are highly variable (Burchard et al., 2018; Chen and de Swart, 2018). Generally, cohesive sediments (mud) are observed near the river mouth, and permeable sediments (sand) dominate in the outer plume area. Accordingly, the mean grain size of the sediment particles continuously increases from the river mouth to the adjacent ocean (Bian et al., 2013). Concomitantly, the origin and concentration of benthic substrates, such as OC and N, varied from the river mouth (high levels, terrestrial origin) to the oceanic area (low levels, pelagic origin; Gao et al., 2008). This strong spatial discrimination of substrates is expected to condition benthic microbial biogeography and related metabolic reactions. Nevertheless, the potential linkage between substrates and microbial community diversity and biomass in the river-sea continuum is still poorly understood there.

A few studies on the diversity and abundance of the microbial community in the Changjiang River plume area have been conducted to date. For instance, a significant change in the biomass of pico-sized autotrophs and heterotrophic bacteria, as well as microbial diversity in the area, was found before and after the construction of the Three Gorges Dam (Jiao et al., 2007), suggesting the instant response of benthic microbial community diversity and biomass to environmental setting changes (e.g., water temperature and the transport of dissolved nutrients). The dominant phylum was observed to be Proteobacteria after analyzing eight sediment samples outside of the river mouth (Feng et al., 2009). The benthic microbial biomass and taxonomic composition, dominated by nitrifiers (Dang et al., 2008), were also recorded in the hypoxic waters at the 24 isohaline from the continental shelf region between 121°E and 124°E (Liu et al., 2011; Ye et al., 2016). Though their investigations offer a view on the microbial biogeography in the continental shelf, two fundamental research questions remain due to the limited spatial coverage of previous research work: (1) Is there any spatial distribution pattern of the benthic microbiota (community diversity, biomass and metabolic functions) coupled with the transport of the CDW? (2) Is there any linkage between sediment substrate originated from the Changjiang River/adjacent seas and microbial community structure? The limited microbial information in the estuary and adjacent sea may hamper the in-depth understanding of the biogeochemical role played by sediment microorganisms in the area. This study hypothesized that spatial variations of sediment microbial community diversity and biomass are strongly determined by the spread of the Changjiang River plume, which in turn determines the spatial distribution of riverine and pelagic particle inputted to the sediment.

2 Materials and methods

2.1 *Sample collection*

An oceanographic campaign was conducted from the 7th to the 22nd of March 2018 in the area affected by the Changjiang River plume onboard the R/V *Kexue III*, covering a survey area from 29°N to 33°N and from 121°E to 124°E (Figs 1a and b). The sampled region is locus of the confluence of the Changjiang River runoff and seawaters transported by the Yellow Sea Coastal Current from the north (stronger during winter, average water temperature 8°C and average salinity 33 during this survey) and by the Taiwan Warm Current (the branch of Kuroshio Current) from the south (stronger during summer, average water temperature 16°C and average salinity 34 during this survey). Generally, the Taiwan Warm Current intrudes into the shelf along the 50 m isobath and its water frequently reaches Changjiang River mouth (Jiang et al., 2021b). During the cruise, water temperature, salinity, turbidity and chlorophyll *a* in the water column were measured at each sampled site with a conductivity-temperature-depth (SBE 911, Sea-Bird Co.) unit and a fluorescence detector. Surface sediment samples, 48 in total, were collected using a box corer (30 cm × 30 cm sampling area). Undisturbed, surface sediment samples (0–2 cm depth) were rapidly transferred from the box corer into sterilized bags and stored onboard at −20°C. The samples were sent to the laboratory after the cruise and stored at −80°C until analysis.

2.2 *Sediment physicochemical analyses*

Sediment samples were placed in glass petri dishes and then dried in an oven at 60°C until reaching a constant weight for subsequent laboratory analyses (Jiang et al., 2018a). Sediment OC content was determined on an elemental analyzer (Vario EL III, Elementar Analysensysteme GmbH) after incubating samples with 1 mol/L hydrochloric acid for 24 h to remove inorganic frac-

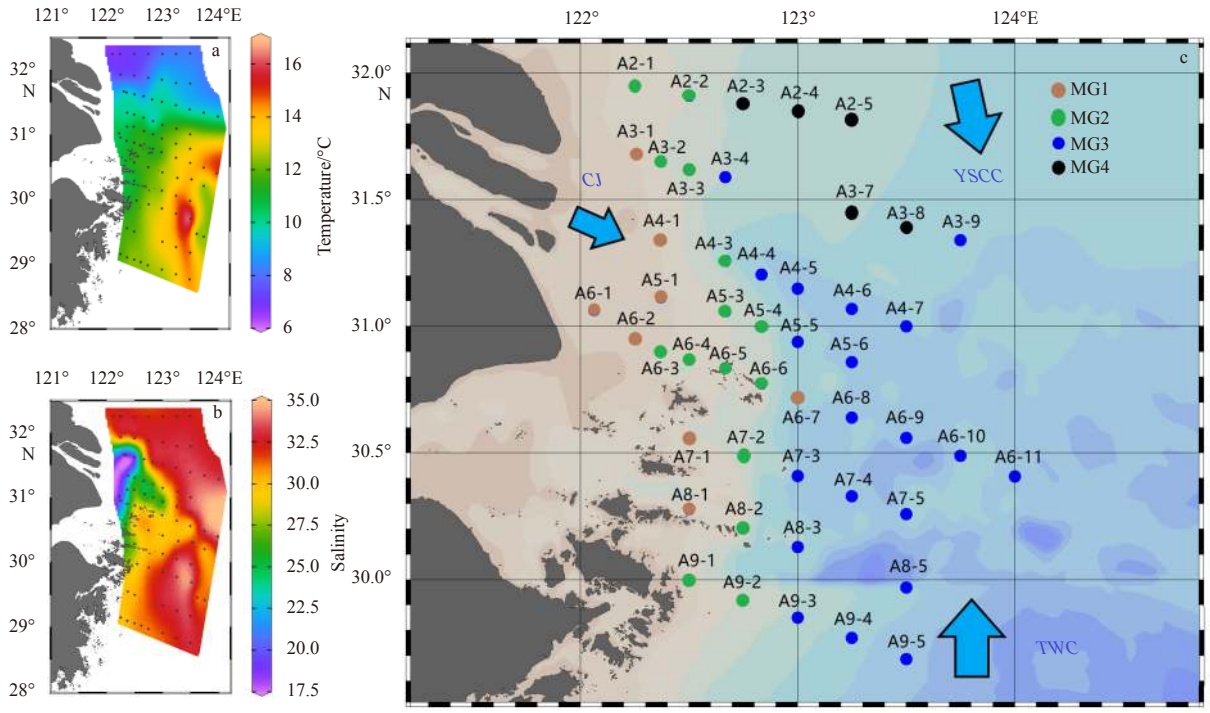

Fig. 1. Spatial distributions of temperature (a) and salinity (b) in surface waters (1 m below sea surface) in the continental shelf affected by the Changjiang River plume during March 2018 as measured with CTD vertical profiles. Dots represent CTD measurement sites. Spatial distribution of the 48 sediment samples collected in the continental shelf affected by the Changjiang River plume in March 2018 (c). The Changjiang River outflow (CJ), Taiwan Warm Current (TWC) and the Yellow Sea Coastal Current (YSCC) are schematically represented based on Kim et al. (2018).

tions (Jiang et al., 2020). TN and S contents (including both inorganic and organic fractions) in the sediment were quantified using the same equipment via the high temperature catalysis method. The sediment inorganic phosphorus (IP) content was extracted with 1 mol/L hydrochloric acid overnight (Aspila et al., 1976). The extraction solution was neutralized with a 1 mol/L sodium hydroxide solution to a pH range of 6 to 8. The P concentration in the neuralized solution was quantified with a flow injection analyzer (SKLAR San++ system, Netherlands) and IP content in the sediment samples was estimated according to the solution concentration and the amount of sediment used. Sediment particle size and size fractions (clay: silt: sand) were measured on a grain size analyzer (Colter LS 100Q). Particle sizes >63 nm were identified as sandy while particle sizes <2 nm were attributed to clay (Wu et al., 2019).

2.3 *DNA extraction and 16S rDNA gene amplification*

From each sample, approximately 0.25 g of sediment was used for total DNA analysis following the procedure of the DNeasy PowerSoil Kit (Qiagen, Germany) in biological safety cabinets. Primers of 341F (5′-CCTAYGGGRBGCASCAG-3′) and 806R (5′-GGACTACNNGGGTATCTAAT-3′) targeted for V3-V4 regions of microbial 16S rDNA genes were used to investigate the microbial diversity (Yu et al., 2005). The 20 μL PCR reaction mixture for V3-V4 amplification contained 0.2 μmol/L of each primer, 250 μmol/L deoyxnucleoside triphosphate (dNTP), 5×FastPfu buffer 5 μL, 1 U FastPfu Polymerase (TransGen Biotech) and 10 ng DNA. The PCR cycling parameters consisted on an initial denaturation (5 min at 95°C), 27 cycles of 30 s at 95°C, 30 s at 55°C, and 45 s at 72°C, and 10 min at 72°C. The PCR fragments were extracted from 2% agarose gels and purified with the FastPure gel DNA extraction mini-Kit (Vazyme Biotech Co., Ltd) according to the manufacturer's instructions.

2.4 *Library construction and sequencing*

The purified PCR products were quantified using Qubit®4.0 (Life Technology), and the KAPA Hyper Prep Kit (Roche) was used for the 16S rDNA gene amplicon library construction. The library was paired-end sequenced (2×300 bp) on an Illumina Miseq system (Illumina) according to standard protocols (Liang et al., 2019). The raw reads were submitted to the NCBI Sequence Read Archive (SRA) database with the submission number SUB5200200 and the accession number from SRR8663111 to SRR8663158.

2.5 *Raw read analysis and Operational Taxonomic Units (OTUs) classification*

The obtained fastq files were demultiplexed with the barcode sequences adapted to the primers using the atlas-utils demultiplex subcommand in biostack suits (version 0.0.1, https://github.com/jameslz/biostack-suits/releases). Bases with a score <3 at the start and the end of the reads were abandoned and reads with a continuous low-quality (score <5) 4 bp or shorter than 150 bp were truncated or abandoned. The USEARCH fastq_mergepairs command (version 9.2.64) with default parameters was used to merge the paired-end reads (Edgar and Flyvbjerg, 2015). Besides, reads which could not be merged or with more than 2 mismatches in the primer area were discarded. The primer sequences in the obtained merged reads were trimmed.

The OTUs were clustered at 97% identity cutoff using USEARCH UPARSE, and the chimeric sequences were abandoned based on the UPARSE pipeline analysis (Edgar, 2013). The

USEARCH SINTAX algorithm was used to analyze the phylogenetic affiliation of the obtained 16S rRNA gene sequences with the RDP training set (version v16) 16S rRNA database as the reference and 0.8 as the confidence threshold (Cole et al., 2014; Edgar, 2016). The OTUs annotated as mitochondrial or chloroplast rRNA gene fragments were abandoned.

2.6 *Alpha- and Beta-diversity analyses*

The USEARCH alpha_div was used to reveal diversity indices of the 48 samples, including the Richness, Chao1, Simpson, Shannon, Dominance, and Equitability parameters (Edgar, 2010). The QIIME software (version 1.9.1) was used to calculate the rarefaction curve based on the OTU table (Caporaso et al., 2010b; Kuczynski et al., 2011; Navas-Molina et al., 2013). The OTU table was normalized with the smallest tags number in all the samples. The required phylogenetic tree of representative OTU sequence was generated using PyNAST algorithm (Caporaso et al., 2010a). The normalized OTU table and the phylogenetic tree was used to calculate Bray-Curtis distance, weighted UniFrac, and unweighted UniFrac to reveal the beta diversity of the samples. The distance matrix between OTUs was used for similarity analysis (ANOSIM). The unweighted pair-group method with arithmetic means (UPGMA) was analyzed with the UPGMA cluster method in the R software, to identify the microbial taxonomic distribution of the samples. The principal co-ordinates analysis (PCoA) in QIIME was used to examine the differences in these 48 microbial communities (Caporaso et al., 2010b). PCoA figures were generated with the Vegan 2.4.2 package in the R environment. Unweighted PCoA plots were applied to visualize the overall differences in microbial communities among samples. The color-mapped PCoA plots were used to enable the visualization of the differences between microbial communities and environmental factors. The ANOSIM test was conducted in the R environment with the Vegan package (Li et al., 2017). The statistical redundancy analysis (RDA) was performed at the OTU-level using the RDA function in the Vegan package. Several collinear environmental factors were removed during the analyses. The raw OTU count table was normalized using the decostandfunction Vegan Package. The ggcord R package (version 1.0.0) was used for the visualization of the RDA results. The network was used to explore microbial co-occurrence, and the program Gephi 0.9.2 was used for network visualization. The top 101 OTUs with relative abundance >0.15% were selected. The selection standard for key OTU co-occurring relationship analysis was Spearman's ρ>0.6 and p<0.01, including both positive and negative correlations (Jiao et al., 2016). The OTUs which have strong interactions with other OTUs in the network were identified as the keystone taxa (Banerjee et al., 2018).

3 Results

3.1 *Microbial community analyses*

The sequence numbers assigned to the kingdom varied from 30 776 to 57 846 in the 48 analyzed samples, with an average sequence number of 48 050±7 593 (Table S1). A total of 2 306 418 high-quality bacterial 16S rRNA V3-V4 gene fragments and 12 581 OTUs were obtained from the 48 samples. OTU numbers in each sample ranged from 1 812 to 4 305 with a mean value of 3 341±504 (Table S1 and Fig. S1). The Good's coverage of the 48 samples was 0.96±0.008 and the richness parameter was similar to the Chao1 parameter, suggesting that most microbes were recovered (Table S1).

At the phylum-level, the top 3 most abundant phyla were Proteobacteria, Acidobacteria and Actinobacteria, accounting on average for 49.2%±10.7%, 6.4%±1.6% and 4.6%±1.7% of the abundance, respectively. Approximately 22.9%±8.9% sequences couldn't be precisely identified, revealing the presence of novel microbes in these sediments (Fig. 2a). For another 36 phyla, their relative abundance was less than4%. At the genus-level, 84.5%±4.8% of the total sequences were assigned to unknown genera (Fig. 2b). For the sequences which can be assigned at the genus level, only *Nitrosopumilus* (3.4%±3.7%) and *Gp22* (1.4%±0.6%) showed a composition larger than 1% of all the sequences (Fig. 2b).

The top 20 most dominant OTUs accounted for 21.6%±4.8% of the bacteria (Table 1). Fourteen of these 20 most dominant OTUs were assigned to Proteobacteria. Most OTUs were similar to the 16S rRNA gene fragments previously identified in the marine environment, and the closest 16S rRNA sequences of all the top 20 dominant OTUs have been recovered before (Table 1). For the top 20 most dominant OTUs, 17 of them show less than 97% identity with known isolates, indicating that the majority of these OTUs are currently uncultured (Table 1). In terms of metabolic functions, the most abundant microbe (OTU_2 *Chromatiales*) might be involved in S transformations (Fig. 2c). The biogeochemical roles involved in the remaining OTUs also included transformations of N and C. For instance, OTU_1 and OTU_50 would be the *Nitrosopumilus* which performs the transformation from NH_4^+ to NO_2^- in the nitrification process (Qin et al., 2017). OTU_5 might be *Pelobacter venetianus*, which participates in the degradation of high-molecular-weight organic matter, such as polyethylene glycol (Schink and Stieb, 1983). OTU_18 would be *Vibrio splendidus*, a pathogenic bacterium in aquaculture (Løvdal et al., 2008).

3.2 *Microbial classification*

Based on the Bray-Curtis distance calculation in the UPGMA analysis, the 48 sediment samples can be classified into 4 clusters at the phylum-level (Fig. 2a), and identified as MG1, MG2, MG3 and MG4. Among these 4 groups, ANOSIM revealed that the inter-group difference was greater than the intra-group difference (Fig. S2; Leung et al., 2016)., reinforcing the rationality and reliability of cluster identification. In the MG1 group, Proteobacteria accounted for 32.7% of all the microbes, and the top 9 phyla accounted for less than 60% of all microbes on average. Moreover, all samples in MG1 contained high abundance of Crenarchaeota (4.8%), including several uncultured mesophilic Crenarchaeota (Könneke et al., 2005). Approximately 37.4% of the microbes in MG1 were assigned to unknown phyla. In the MG2 group, Proteobacteria composes 56.1% of all the microbes and only 17.5% of the microbes were assigned to unknown phyla. Proteobacteria was also the dominant phylum in MG3. Compared with other groups, the MG3 group contains more Thaumarchaeota microbes but less Firmicutes and Euryarchaeota. MG4 was dominated by Proteobacteria. At the genus-level, differences of abundance were frequently observed in group pairs (Fig. S3), such as the abundance of *Nitrosopumilus* and *Gp22* (Fig. 2b).

Most top 20 OTU distributions showed significant differences among the identified sample groups (Table S2), such as OTU_2 distribution between MG1 and MG2 or OTU_2 distribution between MG1 and MG3 (Fig. 2c). The alpha diversity of these 4 groups is outlined in Table 2. Fewer OTUs in the MG1 were observed (Richness) compared to the other 3 groups. The magnitude of the Chao1 parameter of MG4 was smaller than the other 3 groups. The Shannon_2, Simpson, Dominance and Equitability parameters in MG4 were also the lowest identified (Table 2 and Fig. S1).

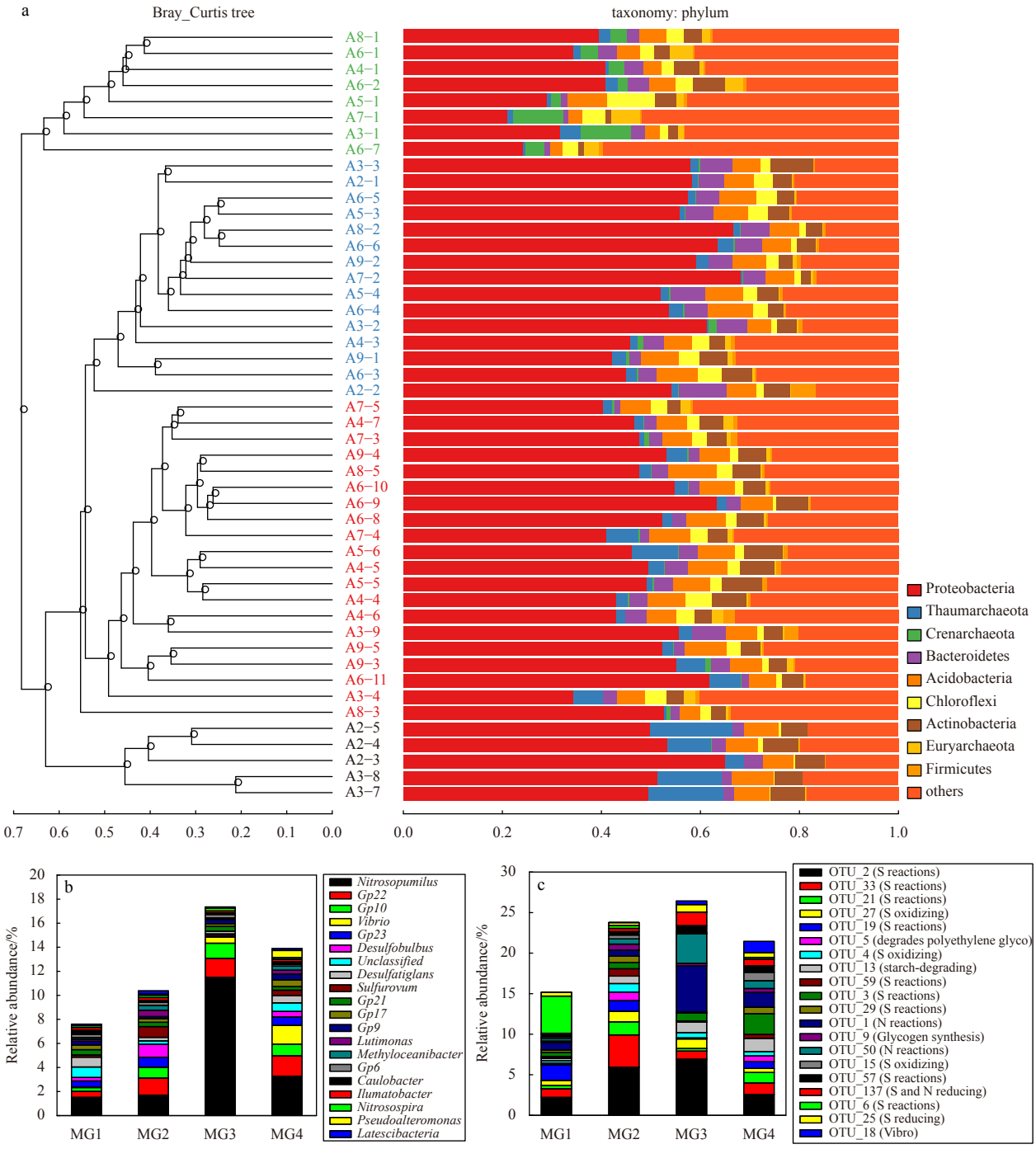

Fig. 2. UPGMA phylogenetic tree based on Bray-Curtis distance combined with phylum-level species distribution (a); the mean abundance of genus and OTUs in MG1, MG2, MG3 and MG4 groups (b and c).

3.3 *Microbial network*

The top 101 OTUs were selected to determine microbial co-occurrence in the four identified groups (Fig. 3). Besides unknown phyla, the OTUs were assigned to 8 phyla with Proteobacteria as the most abundant accounting for 67.3% of the total OTUs. In MG1, the co-occurrence mainly occurred in Proteobacteria, Actinobacteria and Bacteroidetes species (Fig. 3a), revealing the presence of approximately 20 keystone taxa. In MG2 and MG4, nearly all the OTUs showed a high co-occurrence relationship, especially with strong connections between OTUs from Proteobacteria and OTUs from unknown phyla (Figs 3b and d). Accordingly, the quantity of keystone taxa increased. In contrast, OTUs in MG3 were loosely connected (Fig. 3c). Each group contained more than 10 keystone taxa. Notably, the keystone taxa varied among groups, and not all the abundant OTUs in each group were identified as the keystone taxa.

3.4 *Sediment proprieties and relationships with microbial diversity*

Sediment parameters are outlined in Table 3, with marked differences in OC, TN and S contents among the 4 identified groups, revealing different sources of microbial substrates to the

Table 1. Distribution of the top 20 most dominant OTUs, the closest uncultured bacteria 16S rRNA gene fragment and the closest cultured bacteria to these dominant OTUs

	MG1	MG2	MG3	MG4	Closest uncultured bacteria (accession numbers)	Identity	Closest cultured bacteria (accession numbers)	Identity
OTU_2	2.21%±0.99%	5.92%±1.64%	6.92%±1.38%	2.56%±0.66%	uncultured gamma proteobacterium (KU173695.1)	100%	*Woeseia oceani* strain XK5 (NR_147719.1)	96%
OTU_33	1.06%±0.51%	4.00%±1.78%	1.00%±0.77%	1.43%±0.48%	uncultured bacterium clone (KM356694.1)	100%	*Thioprofundum hispidum* strain gps61 (NR_112620.1)	96%
OTU_1	0.91%±0.90%	0.74%±0.36%	5.69%±2.51%	1.81%±1.33%	uncultured marine archaeon (KJ504342.1)	100%	*Nitrosopumilus cobalaminigenes* strain HCA1 (NR_159206.1)	99%
OTU_3	0.52%±0.34%	0.79%±0.41%	0.95%±0.05%	2.55%±0.92%	uncultured bacterium (MG949250.1)	100%	*Desulfatiglans parachlorophenolica* strain DS (NR_126176.1)	90%
OTU_13	0.30%±0.20%	0.93%±0.35%	1.28%±0.67%	1.64%±0.60%	uncultured bacterium (MG002285.1)	100%	*Sandaracinus amylolyticus* strain NOSO 4 (NR_118001.1)	89%
OTU_21	0.43%±0.29%	1.60%±0.47%	0.32%±0.27%	1.29%±0.43%	uncultured bacterium (KX097260.1)	100%	*Desulfobulbus propionicus* strain DSM 2032 (NR_074930.1)	93%
OTU_19	1.93%±1.20%	1.31%±0.73%	0.05%±0.04%	0.83%±0.41%	uncultured Chloroflexi bacterium (GU061267.1)	100%	*Thermomarinilinea lacunifontana* strain SW7 (NR_132293.1)	90%
OTU_50	0.30%±0.22%	0.64%±0.40%	3.63%±1.50%	0.96%±0.70%	uncultured marine group I crenarchaeote (JN590160.1)	100%	*Nitrosopumilus ureiphilus* strain PS0 (NR_159208.1)	97%
OTU_6	4.59%±3.39%	0.36%±0.47%	0.01%±0.01%	0.22%±0.30%	uncultured archaeon (KX952634.1)	100%	*Thermogladius calderae* strain 1633 (NR_148751.1)	85%
OTU_27	0.61%±0.42%	1.32%±0.24%	1.18%±0.96%	0.50%±0.32%	uncultured bacterium (JN621386.1)	99%	*Thiohalomonas nitratireducens* strain HRHd 3sp (NR_043974.1)	93%
OTU_5	0.21%±0.19%	1.06%±0.72%	0.08%±0.08%	0.72%±0.29%	uncultured bacterium (KM203552.1)	100%	*Pelobacter venetianus* strain Gra PEG 1 (NR_044779.1)	93%
OTU_137	0.19%±0.1%	0.40%±0.20%	1.68%±0.73%	0.82%±0.46%	uncultured bacterium (EU491352.1)	99%	*Thioprofundum lithotrophicum* strain 106 (NR_112829.1)	94%
OTU_4	0.28%±0.19%	1.04%±0.42%	0.66%±0.50%	0.53%±0.41%	uncultured gamma proteobacterium (KR086607.1)	100%	*Thiohalobacter thiocyanaticus* strain HRh1 (NR_116699.1)	93%
OTU_29	0.29%±0.09%	0.77%±0.37%	0.15%±0.06%	0.82%±0.30%	uncultured bacterium (KP292396.1)	100%	*Desulfonema magnum* str. Montpellier strain 4be13(NR_025990.1)	93%
OTU_15	0.21%±0.20%	0.48%±0.28%	0.10%±0.17%	1.05%±0.70%	uncultured bacterium (HM598581.1)	100%	*Thermomarinilinea lacunifontana* strain SW7 (NR_132293.1)	89%
OTU_18	0.01%±0.01%	0.00%±0.00%	0.43%±0.40%	1.38%±0.47%	no data	ND	*Vibrio splendidus* strain CH-105 (MH713000.1)	100%
OTU_57	0.27%±0.12%	0.42%±0.12%	0.89%±0.22%	0.80%±0.33%	uncultured bacterium (KX957641.1)	100%	*Desulfosarcina alkanivorans* strain PL12 (NR_157797.1)	93%
OTU_59	0.22%±0.13%	0.90%±0.29%	0.16%±0.19%	0.47%±0.23%	uncultured bacterium (KR825168.1)	100%	*Desulfobulbus propionicus* strain DSM 2032 (NR_074930.1)	91%
OTU_25	0.44%±0.65%	0.35%±0.08%	0.92%±0.53%	0.58%±0.19%	uncultured bacterium (EU734975.1)	100%	*Thermodesulfovibrio aggregans* strain TGE-P1 (NR_040795.1)	85%
OTU_9	0.18%±0.10%	0.74%±0.25%	0.33%±0.25%	0.49%±0.14%	uncultured bacterium (KC631592.1)	100%	*Pseudohaliea rubra* strain CM41_15a (NR_044426.1)	96%

Table 2. The alpha diversity of the obtained four microbial groups in the sediments of the continental shelf affected by the Changjiang River plume

	Richness	Chao1	Shannon_2	Simpson	Dominance	Equitability
MG1	3 337±386	3 338.49±386.00	9.38±0.50	0.007 7±0.005 0	0.990±0.005	0.80±0.04
MG2	3 463±495	3 464.57±495.00	9.20±0.40	0.009 1±0.003 0	0.990±0.003	0.78±0.03
MG3	3 391±516	3 392.54±516.00	9.38±0.30	0.006 8±0.005 0	0.990±0.005	0.80±0.03
MG4	2 789±397	2 791.24±397.00	8.55±0.30	0.014 0±0.004 0	0.980±0.004	0.75±0.02

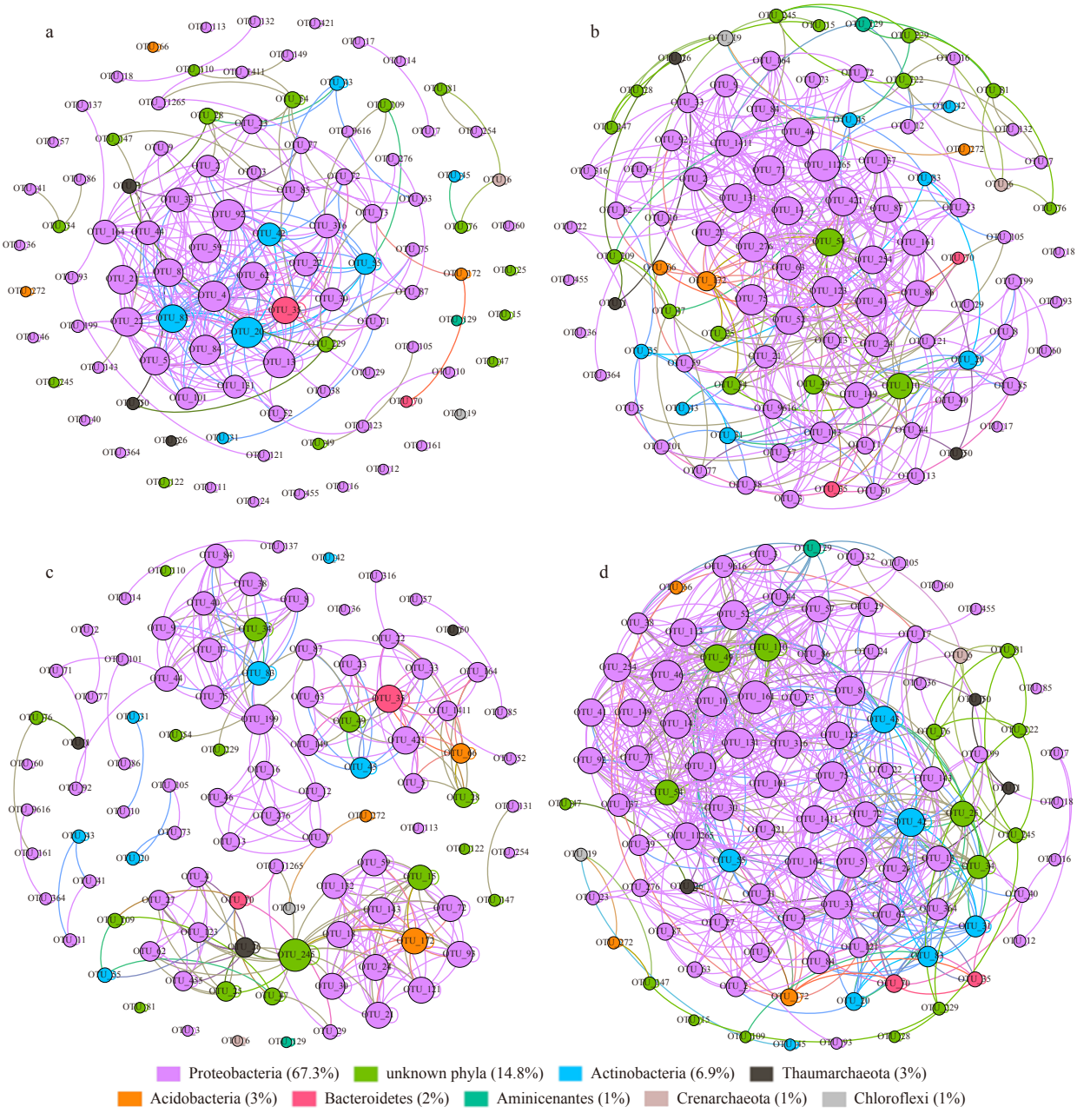

Fig. 3. Network of co-occurring OTUs in MG1 (a), MG2 (b), MG3 (c) and MG4 (d), based on correlation analysis. The selection standards for strong and significant correlation are Spearman's ρ>0.6 and p<0.01, respectively. The size of each node is proportional to the relative abundance of each OTU in the network; the color and thickness of each connection between two nodes (edge) are proportional to the value of Spearman's correlation coefficients. The OTUs assigned to the same phylum were marked with the same color.

sediment. At the OTU-level, the PCoA plots based on unweighted UniFrac distance showed that the majority of samples from the same group were clustered, with several samples from MG1 and MG2 overlapping (Fig. 4). Overall, OC, sediment N, S, and clay contents manifested a continuous distribution of the four identified groups (1 to 4) along the two first components of the PCoA (low

Table 3. Average sediment organic carbon (OC), total nitrogen (TN), sulfur (S) and inorganic phosphorus (IP) contents together with sediment particle sizes (MPS) in the four microbial groups identified through Bray-Curtis distance

	OC content/%	TN content/%	S content/%	IP content/(μmol·g^{-1})	MPS/μm	Clay content/%	Silt proportion/%	Sand proportion/%
MG1	0.5±0.1	0.1±0.0	0.38±0.02	17.8±3.1	9.1±2.7	30.4±4.5	64.0±3.6	5.6±4.3
MG2	0.5±0.2	0.1±0.0	0.28±0.04	18.5±4.4	12.8±8.4	27±5.9	63.3±6	9.7±10.6
MG3	0.1±0.0	0.0±0.0	0.14±0.00	14.9±3.3	239.0±43.4	4.8±2.3	9.1±4.9	86.1±7.1
MG4	0.3±0.1	0.1±0.0	0.22±0.04	16.4±6.0	76.8±54.4	18.7±4.0	30.0±8.4	51.3±11.7

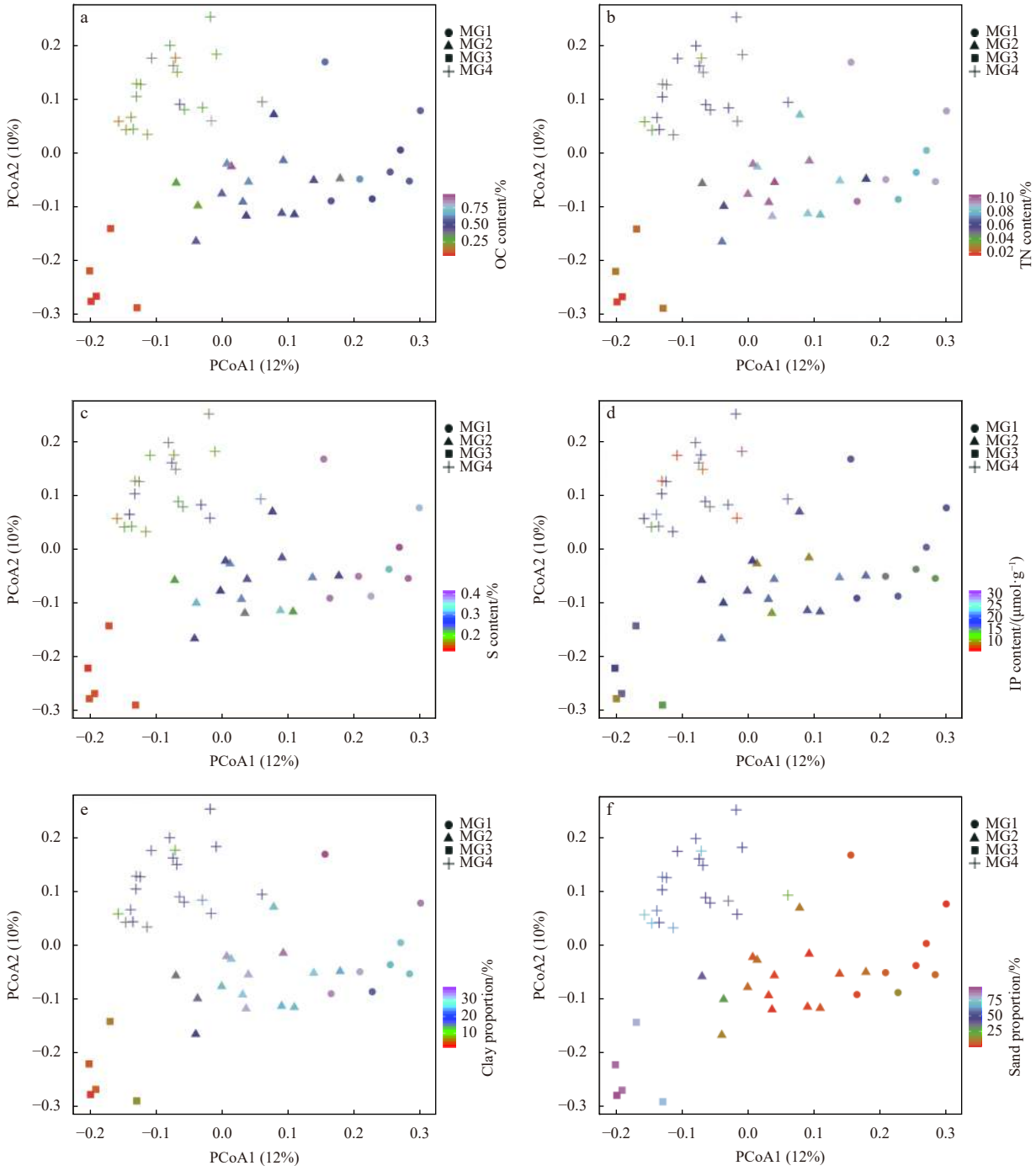

Fig. 4. Unweighted unifrac PCoA plots visualizing community dissimilarities and variations of environmental factors. OC represents organic carbon; TN, total nitrogen; S, sulfur; IP, inorganic phosphorus. The color code denotes the target environmental variable level.

to high component 1, and low to high component 2); while sand content showed an antagonistic trend (Fig. 4). Inorganic phosphorous displayed an unclear trend. The RDA analysis further supported the connections found in the PCoA tests (Fig. 5). Among all the factors tested, OC, TN, S, and silt contents in sediments had significant effects (p<0.01) on the microbial distribution (Fig. 5).

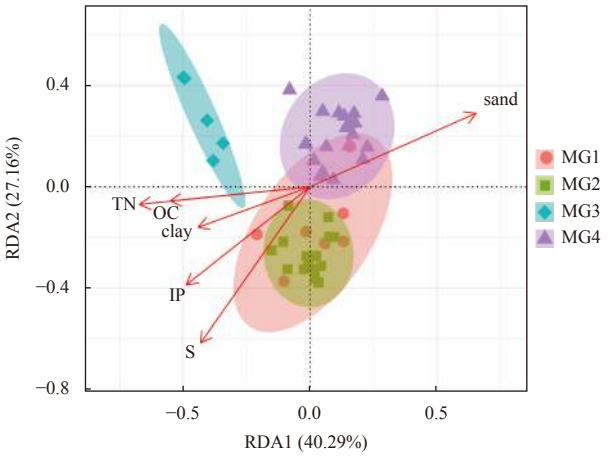

Fig. 5. Relationships of overall community structure and environmental factors obtained through RDA analysis, including contents (according to mass fraction) of organic carbon (OC), total nitrogen (TN), sulfur (S), inorganic phosphorus (IP), and proportions of clay and sand in the continental shelf samples.

4 Discussion

Among the collected sediment samples (48 samples), the most abundant bacterium was assigned to Proteobacteria (49%), which is in line with other studies conducted in the Changjiang River plume area (Ye et al., 2016). In adjacent seas and estuaries, such as the Zhujiang River Estuary (Mai et al., 2018), the South Yellow Sea (Chen et al., 2021) and the East China Sea (Dong et al., 2014), Proteobacteria was also identified as the dominant phylum. In addition, on a global scale, high-abundance of Proteobacteria in both estuarine/marine sediments has been reported, frequently involved in biogeochemical transformations of C, N, and S in the benthic environment (Inagaki et al., 2006; McCaig et al., 1999; Nold et al., 2000). Actinobacteria was the second most abundant phylum in the collected sediments (4.6%). The high abundance of Actinobacteria was also observed in the Yellow Sea (Wei et al., 2018) and Rajang River Estuary, Malaysia (Sia et al., 2019). Actinobacteria are frequently involved in the metabolic production of polyketides and nonribosomal peptides. High abundance of Actinobacteria suggests that sediments in the area of influence of the Changjiang River plume have high potential in the biosynthesis of antibiotics (Gomez-Escribano et al., 2016).

Though these dominant species were observed in all sediment samples, the community structure, especially the taxonomic composition of benthic microbes significantly varied along the continental shelf affected by the river plume. Contrasting with research performed by Feng et al. (2009) that showed unclear spatial distribution patterns of the benthic microbial community in the Changjiang River plume area, benthic microbial community studied here can be grouped into four different clusters via the UPGMA analysis using Bray-Curtis distance. These groups showed a significant difference in taxonomic composition between each other (Fig. S2) and a clear spatial pattern distributed from the Changjiang River mouth to the outer plume area, following the spatial distribution of environmental drivers derived from the interaction between the transport of terrestrial material by the Changjiang River and sea currents from the East China Sea and the Yellow Sea (Fig. 1c). Salinity and temperature are deemed to be key factors shaping the microbial community in estuaries (Sunagawa et al., 2015). In this study, the salinity in the waters near bottom sediments was ca. 32 in the majority of sites because of the low discharge rate of Changjiang River and wind-induced seawater intrusion during winter-early spring (Fig. S4). Near-bottom water temperature ranged from 6°C to 15°C from the north to the south and displayed a decreasing trend along the latitude increase (Fig. S4), which was different from the identified spatial pattern of taxonomic composition (Fig. 1c). Consequently, the influence of these physical factors on the spatial distribution of the benthic microbial community in the studied coastal region seems limited.

Apart from the Site A6-7, samples grouped in MG1 are located in the vicinity of the Changjiang River mouth (Fig. 1c), receiving substantial Changjiang River-borne particles with terrestrial signal throughout the year (Li et al., 2020), evidenced by the high turbidity near the sediment surface during both low and high river discharge periods (Figs S4 and S5). Riverine transport of particles may also introduce Changjiang River-borne microbes in the studied sediments (Dang et al., 2008). Liu et al. (2018) showed that *Planctmyces* and *Pseudomonas* dominate the benthic community in Changjiang River sediments. This significantly contrasts with the microbial composition of group MG1, where Proteobacteria and Creanarchaeota were key phyla (excluding unknown species). Such difference reveals a rearrangement of the dominant species in the fresh-to-saline water transition environments despite potentially receiving allochthonous microbes. Furthermore, in MG1, the abundant OTUs were OTU_6 (*Thermoprotei*), OTU_2 (*Chromatiales*) and OTU_19 (*Anaerolineaceae*). All of them are predicted to participate in sediment S turnover (Fig. 3c) and represent keystone taxa in the benthic metabolism. Concurrently, high-level sediment S content was obtained in these sediment samples near the river mouth (Table 3). In addition, S enrichment of the suspended particles transported by the river was previously reported, which can be used as electron donor thus supporting microbial metabolism via oxidative reactions (Li et al., 2011). In parallel, high-concentrations of dissolved dimethylsulfoniopropionate (DMSPd) and dissolved dimethylsulfoxide (DMSOd) are frequently observed in the river mouth (Gao et al., 2017), likely to be products of the oxidation of land-derived S. Near the river mouth, due to the interactions of shallow depths and tidal forces, intense sediment resuspension occurs (Zhu et al., 2017), which enhances oxidative reactions via increasing the contact between sediment microbes and dissolved oxygen in the overlaying waters. Furthermore, seawater intrusion in the saltwater wedge introduces sulfate in the river mouth area. Coupled with terrestrial OC from the river plume, a fraction of sulfate is likely reduced to sulfide (He et al., 2015). The combination of these factors and reactions may explain the enrichment of microbes specialized in S processing in surface sediments near the river mouth (correlations from the PCoA and RDA analyses), which greatly shapes the benthic microbial composition there. The significance of S content on microbial composition could also be witnessed at the A6-7 site, i.e., a site belonging to the MG1 group but far from the river mouth. This site is characterized by much higher S content (0.38%) than the mean levels found in MG2 (Table 3). Apart from S reactors, in MG1, 4 OTUs identified as Actinobacteria were outlined in the center of the metabolic net (Fig. 3a). Considering that the Changjiang River watershed holds a human population of more than 300 million and that the river mouth receives the direct anthropogenic outflow from a megacity (Shanghai larger than 20 million population; Zhang et al., 2021), the high abundance of Actinobacteria in MG1 may play a role in the removal of terrestrial organic contaminants from human industries (Hu et al., 2013; Piza et al., 2004).

In the region where the MG2 group was identified, OTU_2 (Gamma Proteobacterium, *Chromatiales* strain) was the dominant species, increasing abundance compared to MG1 (from 2.2% in MG1 to 5.9% in MG2). In addition, OTU_33 (another *Chromatiales* strain) also markedly increased in MG2 compared to MG1, from 1.1% to 4.0% (Fig. 2 and Table 1). This increase suggests an enhancement of oxidative reactions, which links to the continuous suspension of sediment particles in the oxygen-saturated overlying water. In particular, the location of the maximum turbidity zone frequently shifts between the outer region of MG1 and the entire MG2 region, depending on the seasonal riverine discharge rate. The high turbidity of the overlying water (Figs S4 and S5), likely resulting from flocculation of riverine materials and particle resuspension driven by seawater intrusion (Zhang et al., 2020a), benefits oxidative reactions on sediment particle surfaces, especially the S-oxidizing reactions carried by Chromatiales (Cleary et al., 2017). This seems to be a major pathway sustaining the local benthic metabolism (Audry et al., 2007). The increase in S-oxidizing potential may also result from the decrease of terrestrially derived labile organic content since this portion might be preferentially consumed by microbiota in MG1 prior to reaching MG2. Compared with the flourished microbial S reaction pathways, OTU_19 and OTU_6 markedly decreased in this region compared to MG1, especially OTU_6 (*Thermogladius calderae*, from 4.6% to 0.36%). Based on laboratory culture experiments carried by Kochetkova et al. (2016), *Thermogladius calderae* is highly selective on carbon substrate utilization. Considering the carbon consumption sequence of MG1 and MG2, the decline of OUT_6 in MG2 could also be interpreted as the result of changing sediment organic matter quantity and quality. To conclude, the OTU co-occurrence between MG1 and MG2 was similar, and the keystone taxa in the microbial community of both regions were identified as dependent on S substrates (Fig. 3).

The identified group MG3 showed a significant variation in sediment microbiota at both the phylum-level and the genus-level compared to the other inner-most two groups (Fig. 2). For microbial distribution at the OTU-level, OTU_2 was still the most abundant OTU in the microbial community (Fig. 2c). However, abundances of other S-related microbes significantly dropped (Table 1), which was parallel to the decrease in S content in the sediment (Table 3). Alternatively, abundances of *Nitrosopumilus* (OTU_1 and OTU_50) markedly increased (Figs 2b and c). Moreover, OTU co-occurrence revealed that the dominant S-based, benthic metabolism weakened. In this region, the turbidity in the surface water sharply decreased with low quantity of terrestrial particles (Chen et al., 2008; Fig. S4), while the water from the Taiwan Warm Current and the Yellow Sea significantly intrudes into the region (Fig. S1). These sea currents are rich in pelagic particles, including blooms of *Prorocentrum donghaiense* during the spring and early summer (Wang et al., 2020) and blooms of *Skeletonema costatum* during the summer and early autumn (Bian et al., 2013; see the fluorescence peaks in Fig. S5, including a bloom of *Skeletonema costatum* in July 2017). As a response, the benthic microbial metabolism shifted from S-based (terrestrial particles, S enriched) to N-based (pelagic sources). *Nitrosopumilus* conducts the oxidation of NH_4^+ to NO_2^- during the autotrophic nitrification process, relying on the ammonium production during the benthic decomposition of phytoplankton detritus sinking from surface waters, especially during algae blooms (Ye et al., 2016). During benthic mineralization and ammonification processes, NH_4^+ is produced from labile organic N, such as amino acids, and then subject to nitrification in oxic environments (Jiang et al., 2019). N-enriched pelagic organic matter thus fuels a cascade of benthic microbial reactions including the denitrification process (increased abundance of OTU_137; nitrite reducer), tightly linked to nitrification in benthic sediments (Liu et al., 2019). The correlation between sediment OC/N and microbial community structure is supported by the RDA analysis performed and continuously increased (low to high) along the two axes of the PCoA plots. Compared with the MG1 and MG2 regions, sediment OC and N in MG3 was much lower. This may be based on the rapid turnover of pelagic organic matter in the sediments due to its lability, thus sustaining the entire microbial community there. Accordingly, the microbial network in MG3 was significantly different from the pattern observed in MG1 and MG2 zones (loosely connected, several clusters), displaying the multiple selection for substrates during their metabolic reactions.

In the MG4 zone, an increase in sediment C and N compared to sediments from the MG3 group was observed, which is similar to the levels found in the Yellow Sea (Hu et al., 2013). This region is occasionally influenced by the outer Changjiang River plume during the summer (June to August), the period of highest riverine discharge (discharge >70 000 m^3/s, Jiang et al., 2021b). During the rest of the year, the area is dominated by the Yellow Sea water masses (high salinity and low temperature, Fig. S4). In this region, abundances of the majority of the OTUs tended to be identical among samples, with OTU_2 presenting the highest records (2.6%). As a result, substantial OTUs were clustered together in the network, creating a dense web (Fig. 3d). This distribution likely reflects the instability of substrate supply because of the geographic location of this group. Specifically, because of the long distance to the river mouth, this region lacks the input of terrestrial particles (Zhang et al., 2020b). S, especially sulfide-metal, might be limited in the MG4 region. In addition, phytoplankton blooms are mainly occurring in the MG3 region due to the relatively high concentration of dissolved nutrients and trace elements transported by the Changjiang River plume (Fig. S5; Chang et al., 2021; Jiang et al., 2021b), suggesting a low input of pelagic organic matter in the MG4 region by comparison. Altogether, substrate inputs in MG4 might be limited on both terrestrial and pelagic sources. Accordingly, the intense recirculation and high efficiency utilization of the limited substrates in the sandy sediments sustain the basic functions of sediment microbiota via active co-metabolism, as previously observed in coastal sediments of an oligotrophic bay (Jiang et al., 2021c).

Interestingly, among the four identified groups, sediment IP content was not identified as an important factor for the benthic microbial distribution in the RDA analyses, though it serves as an essential element for microbial metabolism. For instance, OTU_18 (*Vibrio splendidus*) showed a strong dependence on P in laboratory cultures (Schink and Stieb, 1983). The high storage capacity of P in sediments might be an important reason for this. In the studied sediments, though the measurement of sediment N might not be precise at low concentrations, the C:P and N:P stoichiometry ratios were markedly below Redfield ratios. The high-level P in the sampled sediments likely results from the strong adsorption capability of sediments and subsequent P sequestration (Jiang et al., 2018b). Because of such high-levels, P may not be a limiting element for local benthic metabolism and therefore the linkage of sediment P content with benthic microbial community composition was weak.

The significant correlation obtained between sediment particle size (clay) and microbial structure can be explained by two reasons. On the one hand, small particles have a larger specific surface area, indicating that abundant microniches can be

provided for supporting activities of sediment microbes. On the other hand, there was a strong correlation between particle size and sediment C/N (content ratio). The effects from particle size on the sediment microbial community may be the mirror of influences from the availability of these substrates. Therefore, it is not surprising to find that positive relationship between sediment particle size and microbial structure.

5 Conclusions

The 48 sediment samples collected on the continental shelf affected by the spread of the Changjiang River plume were used to characterize the benthic microbial community and to elucidate its biogeography. From the river mouth to the outer plume, the benthic microbial structure can be clearly classified into 4 clusters at the phylum level. The dominant phylum in all clusters was Proteobacteria. Acidobacteria and Actinobacteria were also frequently observed. The distribution of these benthic microbes can be related to sediment substrate (C, N and S) availability affected by the river plume and ocean currents. In regions close to the river mouth receiving Changjiang River derived particles, S reactions seem to play a dominant role in the microbial metabolism and these microbes (e.g., Thermoprotei and Chromatiales) were assigned to the key taxa in the microbial community. In the outer region, the water turbidity decreased, thus benefiting the growth of phytoplankton. C and N turnover, supported by debris of phytoplankton in the sediment, tended to be the major metabolic pathways. This shift of microbial biogeography is linked to the substrate supply in the river-ocean continuum (riverine particles and debris of phytoplankton), significantly influencing the transformation of nutrients and trace elements though processes such as denitrification or mineralization of organic matter. Accordingly, the detailed characterization of sediment microbiota, including microbial biomass and taxonomic composition, could help to understand the magnitude and spatial distribution of biogeochemical processes in this region such as carbon sequestration, N removal, S oxidation, etc. Besides, this study found abundant Actinobacteria in the study area which harbor abundant/diverse natural product biosynthetic genes/gene clusters. In-depth exploration of these synthetic pathways using metagenomics is highly recommended.

Acknowledgements

We acknowledge Ying Cui in East China Normal University and Guanghui Lin in Tsinghua University for laboratory analyses assistance. We appreciate the team leader (Rencheng Yu) and crew members of the R/V *Kexue III* (supported by Institute of Oceanology, Chinese Academy of Sciences and National Natural Science Foundation of China) for their dedication during oceanographic cruises. We thank DeepBiome Co., Ltd. for bioinformatic assistance. We are thankful to three anonymous reviewers whose comments helped to improve an earlier version of the manuscript.

References

Aspila K I, Agemian H, Chau A S Y. 1976. A semi-automated method for the determination of inorganic, organic and total phosphate in sediments. Analyst, 101(1200): 187–197, doi: 10.1039/AN9760100187

Audry S, Blanc G, Schäfer J, et al. 2007. Effect of estuarine sediment resuspension on early diagenesis, sulfide oxidation and dissolved molybdenum and uranium distribution in the Gironde estuary, France. Chemical Geology, 238(3–4): 149–167, doi: 10.1016/j.chemgeo.2006.11.006

Banerjee S, Schlaeppi K, van der Heijden M G A. 2018. Keystone taxa as drivers of microbiome structure and functioning. Nature Reviews Microbiology, 16(9): 567–576, doi: 10.1038/s41579-018-0024-1

Bertics V J, Ziebis W. 2010. Bioturbation and the role of microniches for sulfate reduction in coastal marine sediments. Environmental Microbiology, 12(11): 3022–3034, doi: 10.1111/j.1462-2920.2010.02279.x

Bian Changwei, Jiang Wensheng, Quan Qi, et al. 2013. Distributions of suspended sediment concentration in the Yellow Sea and the East China Sea based on field surveys during the four seasons of 2011. Journal of Marine Systems, 121–122: 24–35, doi: 10.1016/j.jmarsys.2013.03.013

Brandsma J, Martínez J M, Slagter H A, et al. 2013. Microbial biogeography of the North Sea during summer. Biogeochemistry, 113(1–3): 119–136

Burchard H, Schuttelaars H M, Ralston D K. 2018. Sediment trapping in estuaries. Annual Review of Marine Science, 10(1): 371–395, doi: 10.1146/annurev-marine-010816-060535

Caporaso J G, Bittinger K, Bushman F D, et al. 2010a. PyNAST: a flexible tool for aligning sequences to a template alignment. Bioinformatics, 26(2): 266–267, doi: 10.1093/bioinformatics/btp636

Caporaso J G, Kuczynski J, Stombaugh J, et al. 2010b. QIIME allows analysis of high-throughput community sequencing data. Nature Methods, 7(5): 335–336, doi: 10.1038/nmeth.f.303

Chang Yan, Müller M, Wu Ying, et al. 2020. Distribution and behaviour of dissolved selenium in tropical peatland-draining rivers and estuaries of Malaysia. Biogeosciences, 17(4): 1133–1145, doi: 10.5194/bg-17-1133-2020

Chang Yan, Wu Ying, Zhang Jing, et al. 2021. Effects of algal blooms on selenium species dynamics: A case study in the Changjiang Estuary, China. Science of the Total Environment, 768: 144235, doi: 10.1016/j.scitotenv.2020.144235

Chang Yan, Zhang Jing, Qu Jianguo, et al. 2016. The behavior of dissolved inorganic selenium in the Changjiang Estuary. Journal of Marine Systems, 154: 110–121, doi: 10.1016/j.jmarsys.2015.01.008

Chen Wei, de Swart H E. 2018. Longitudinal variation in lateral trapping of fine sediment in tidal estuaries: observations and a 3D exploratory model. Ocean Dynamics, 68(3): 309–326, doi: 10.1007/s10236-018-1134-z

Chen Lianguo, Tsui M M P, Lam J C W, et al. 2019. Variation in microbial community structure in surface seawater from Pearl River Delta: Discerning the influencing factors. Science of the Total Environment, 660: 136–144, doi: 10.1016/j.scitotenv.2018.12.480

Chen Ye, Li Siqi, Xu Xiaoqing, et al. 2021. Characterization of microbial communities in sediments of the South Yellow Sea. Journal of Oceanology and Limnology, 39(3): 846–864, doi: 10.1007/s00343-020-0106-6

Chen Changsheng, Xue Pengfei, Ding Pingxing, et al. 2008. Physical mechanisms for the offshore detachment of the Changjiang Diluted Water in the East China Sea. Journal of Geophysical Research: Oceans, 113(C2): C02002, doi: 10.1029/2006JC003994

Cleary D F R, Coelho F J R C, Oliveira V, et al. 2017. Sediment depth and habitat as predictors of the diversity and composition of sediment bacterial communities in an inter-tidal estuarine environment. Marine Ecology, 38(2): e12411, doi: 10.1111/maec.12411

Cole J R, Wang Qiong, Fish J A, et al. 2014. Ribosomal Database Project: data and tools for high throughput rRNA analysis. Nucleic Acids Research, 42(D1): D633–D642, doi: 10.1093/nar/gkt1244

Dang Hongyue, Zhang Xiaoxia, Sun Jin, et al. 2008. Diversity and spatial distribution of sediment ammonia-oxidizing Crenarchaeota in response to estuarine and environmental gradients in the Changjiang Estuary and East China Sea. Microbiology, 154(7): 2084–2095, doi: 10.1099/mic.0.2007/013581-0

Dong Yi, Zhao Yuan, Zhang Wenyan, et al. 2014. Bacterial diversity and community structure in the East China Sea by 454 sequencing of the 16S rRNA gene. Chinese Journal of Oceanology and Limnology, 32(3): 527–541, doi: 10.1007/s00343-014-3215-2

Edgar R C. 2010. Search and clustering orders of magnitude faster than BLAST. Bioinformatics, 26(19): 2460–2461, doi: 10.1093/bioinformatics/btq461

Edgar R C. 2013. UPARSE: highly accurate OTU sequences from microbial amplicon reads. Nature Methods, 10(10): 996–998, doi: 10.1038/NMETH.2604

Edgar R C. 2016. SINTAX: a simple non-Bayesian taxonomy classifier for 16S and ITS sequences. bioRxiv. (2016-09-09)[2020-10-13]. http://europepmc.org/article/PPR/PPR33123. doi: 10.1101/074161

Edgar R C, Flyvbjerg H. 2015. Error filtering, pair assembly and error correction for next-generation sequencing reads. Bioinformatics, 31(21): 3476–3482, doi: 10.1093/bioinformatics/btv401

Feng Biwei, Li Xiaoran, Wang Jinhui, et al. 2009. Bacterial diversity of water and sediment in the Changjiang Estuary and coastal area of the East China Sea. FEMS Microbiology Ecology, 70(2): 236–248, doi: 10.1111/j.1574-6941.2009.00772.x

Fournier S, Lee T, Gierach M M. 2016. Seasonal and interannual variations of sea surface salinity associated with the Mississippi River plume observed by SMOS and Aquarius. Remote Sensing of Environment, 180: 431–439, doi: 10.1016/j.rse.2016.02.050

Gao Jianhua, Wang Yaping, Pan Shaoming, et al. 2008. Spatial distributions of organic carbon and nitrogen and their isotopic compositions in sediments of the Changjiang Estuary and its adjacent sea area. Journal of Geographical Sciences, 18(1): 46–58, doi: 10.1007/s11442-008-0046-010.3321/j.issn:0375-5444.2007.09.009

Gao Nan, Yang Guipeng, Zhang Honghai, et al. 2017. Temporal and spatial variations of three dimethylated sulfur compounds in the Changjiang Estuary and its adjacent area during summer and winter. Environmental Chemistry, 14(3): 160–177, doi: 10.1071/EN16158

Gomez-Escribano J P, Alt S, Bibb M J. 2016. Next generation sequencing of actinobacteria for the discovery of novel natural products. Marine Drugs, 14(4): 78, doi: 10.3390/md14040078

Gudasz C, Bastviken D, Steger K, et al. 2010. Temperature-controlled organic carbon mineralization in lake sediments. Nature, 466(7305): 478–481, doi: 10.1038/nature09186

He Hui, Zhen Yu, Mi Tiezhu, et al. 2015. Community composition and distribution of sulfate- and sulfite-reducing prokaryotes in sediments from the Changjiang Estuary and adjacent East China Sea. Estuarine, 165: 75–85, doi: 10.1016/j.ecss.2015.09.005

Hu Shaohua, Herner J D, Robertson W, et al. 2013. Emissions of polycyclic aromatic hydrocarbons (PAHs) and nitro-PAHs from heavy-duty diesel vehicles with DPF and SCR. Journal of the Air & Waste Management Association, 63(8): 984–996, doi: 10.1080/10962247.2013.795202

Ibánhez J S P, Araujo M, Lefèvre N. 2016. The overlooked tropical oceanic CO_2 sink. Geophysical Research Letters, 43(8): 3804–3812, doi: 10.1002/2016GL068020

Inagaki F, Nunoura T, Nakagawa S, et al. 2006. Biogeographical distribution and diversity of microbes in methane hydrate-bearing deep marine sediments on the Pacific Ocean Margin. Proceedings of the National Academy of Sciences of the United States of America, 103(8): 2815–2820, doi: 10.1073/pnas.0511033103

Jiang Shan, Ibánhez J S P, Rocha C. 2018a. Influence of labile dissolved organic matter on nitrate reduction in a seepage face. Environmental Science and Pollution Research, 25(11): 10654–10667, doi: 10.1007/s11356-018-1302-1

Jiang Shan, Jin Jie, Wu Ying, et al. 2021a. Response of nitrate processing to bio-labile dissolved organic matter supply under variable oxygen conditions in a sandy beach seepage face. Frontiers in Marine Science, 8:642143, doi: 10.3389/fmars.2021.642143

Jiang Shan, Jin Jie, Zhang Guosen, et al. 2021b. Nitrate in the Changjiang diluted water: an isotopic evaluation on sources and reaction pathways. Journal of Oceanology and Limnology, 39(3): 830–845, doi: 10.1007/s00343-020-0149-8

Jiang Shan, Kavanagh M, Ibánhez J S P, et al. 2021c. Denitrification-nitrification process in permeable coastal sediments: an investigation on the effect of salinity and nitrate availability using flow-through reactors. Acta Oceanologica Sinica, 40(10): 1–13, doi: 10.1007/s13131-021-1811-5

Jiang Shan, Lu Haoliang, Liu Jingchun, et al. 2018b. Influence of seasonal variation and anthropogenic activity on phosphorus cycling and retention in mangrove sediments: A case study in China. Estuarine, 202: 134–144, doi: 10.1016/j.ecss.2017.12.011

Jiang Shan, Müller M, Jin Jie, et al. 2019. Dissolved inorganic nitrogen in a tropical estuary in Malaysia: transport and transformation. Biogeosciences, 16(14): 2821–2836, doi: 10.5194/bg-16-2821-2019

Jiang Shan, Zhang Yixue, Jin Jie, et al. 2020. Organic carbon in a seepage face of a subterranean estuary: Turnover and microbial interrelations. Science of the Total Environment, 725: 138220, doi: 10.1016/j.scitotenv.2020.138220

Jiao Shuo, Liu Zhenshan, Lin Yanbing, et al. 2016. Bacterial communities in oil contaminated soils: Biogeography and co-occurrence patterns. Soil Biology and Biochemistry, 98: 64–73, doi: 10.1016/j.soilbio.2016.04.005

Jiao Lijing, Wu Jianpeng, He Xiang, et al. 2018. Significant microbial nitrogen loss from denitrification and anammox in the land-sea interface of low permeable sediments. International Biodeterioration & Biodegradation, 135: 80–89, doi: 10.1016/j.ibiod.2018.10.002

Jiao Nianzhi, Zhang Yao, Zeng Yonghui, et al. 2007. Ecological anomalies in the East China Sea: impacts of the Three Gorges Dam?. Water Research, 41(6): 1287–1293, doi: 10.1016/j.watres.2006.11.053

Kim J, Cho H M, Kim G. 2018. Significant production of humic fluorescent dissolved organic matter in the continental shelf waters of the northwestern Pacific Ocean. Scientific Reports, 8(1): 4887, doi: 10.1038/s41598-018-23299-1

Kochetkova T V, Kublanov I V, Toshchakov S V, et al. 2016. *Thermogladius calderae* gen. nov., sp. nov., an anaerobic, hyperthermophilic Crenarchaeote from a Kamchatka hot spring. International Journal of Systematic and Evolutionary Microbiology, 66(3): 1407–1412, doi: 10.1099/ijsem.0.000916

Könneke M, Bernhard A E, de la Torre J R, et al. 2005. Isolation of an autotrophic ammonia-oxidizing marine archaeon. Nature, 437(7058): 543–546, doi: 10.1038/nature03911

Kuczynski J, Stombaugh J, Walters W A, et al. 2011. Using QIIME to analyze 16S rRNA gene sequences from microbial communities. Current Protocols in Bioinformatics, 36(1): 10.7.1–10.7.20, doi: 10.1002/0471250953.bi1007s36

Kuypers M M M, Marchant H K, Kartal B. 2018. The microbial nitrogen-cycling network. Nature Reviews Microbiology, 16(5): 263–276, doi: 10.1038/nrmicro.2018.9

Lefèvre N, Montes F M, Gaspar F L, et al. 2017. Net heterotrophy in the Amazon Continental Shelf changes rapidly to a sink of CO_2 in the outer Amazon Plume. Frontiers in Marine Science, 4: 278, doi: 10.3389/fmars.2017.00278

Leung M H Y, Chan K C K, Lee P K H. 2016. Skin fungal community and its correlation with bacterial community of urban Chinese individuals. Microbiome, 4(1): 46, doi: 10.1186/s40168-016-0192-z

Li Tongtong, Long Meng, Li Huan, et al. 2017. Multi-Omics analysis reveals a correlation between the host phylogeny, gut microbiota and metabolite profiles in cyprinid fishes. Frontiers in Microbiology, 8: 454, doi: 10.3389/fmicb.2017.00454

Li Zhongqiao, Wu Ying, Yang Liyang, et al. 2020. Carbon isotopes and lignin phenols for tracing the floods during the past 70 years in the middle reach of the Changjiang River. Acta Oceanologica Sinica, 39(4): 33–41, doi: 10.1007/s13131-020-1543-y

Li Weijun, Zhou Shengzhen, Wang Xinfeng, et al. 2011. Integrated evaluation of aerosols from regional brown hazes over northern China in winter: Concentrations, sources, transformation, and mixing states. Journal of Geophysical Research: Atmospheres, 116(D9): D09301, doi: 10.1029/2010JD015099

Liang Jiawei, Mai Wenning, Tang Jinfeng, et al. 2019. Highly effective treatment of petrochemical wastewater by a super-sized industrial scale plant with expanded granular sludge bed bioreactor

and aerobic activated sludge. Chemical Engineering Journal, 360: 15–23, doi: 10.1016/j.cej.2018.11.167

Liu Cheng, Hou Lijun, Liu Min, et al. 2019. Coupling of denitrification and anaerobic ammonium oxidation with nitrification in sediments of the Yangtze Estuary: Importance and controlling factors. Estuarine, 220: 64–72, doi: 10.1016/j.ecss.2019.02.043

Liu Min, Xiao Tian, Wu Ying, et al. 2011. Temporal distribution of the archaeal community in the Changjiang Estuary hypoxia area and the adjacent East China Sea as determined by denaturing gradient gel electrophoresis and multivariate analysis. Canadian Journal of Microbiology, 57(6): 504–513, doi: 10.1139/w11-037

Liu Tang, Zhang Anni, Wang Jiawen, et al. 2018. Integrated biogeography of planktonic and sedimentary bacterial communities in the Yangtze River. Microbiome, 6(1): 16, doi: 10.1186/s40168-017-0388-x

Løvdal T, Skjoldal E F, Heldal M, et al. 2008. Changes in morphology and elemental composition of *Vibrio splendidus* along a gradient from carbon-limited to phosphate-limited growth. Microbial Ecology, 55(1): 152–161, doi: 10.1007/s00248-007-9262-x

Mai Yongzhan, Lai Zini, Li Xinhui, et al. 2018. Structural and functional shifts of bacterioplanktonic communities associated with spatiotemporal gradients in river outlets of the subtropical Pearl River Estuary, South China. Marine Pollution Bulletin, 136: 309–321, doi: 10.1016/j.marpolbul.2018.09.013

McCaig A E, Phillips C J, Stephen J R, et al. 1999. Nitrogen cycling and community structure of proteobacterial β-subgroup ammonia-oxidizing bacteria within polluted marine fish farm sediments. Applied and Environmental Microbiology, 65(1): 213–220, doi: 10.1128/AEM.65.1.213-220.1999

Navas-Molina J A, Peralta-Sánchez J M, González A, et al. 2013. Advancing our understanding of the human microbiome using QIIME. Methods in Enzymology, 531: 371–444, doi: 10.1016/B978-0-12-407863-5.00019-8

Nold S C, Zhou Jizhong, Devol A H, et al. 2000. Pacific northwest marine sediments contain ammonia-oxidizing bacteria in the β subdivision of the *Proteobacteria*. Applied and Environmental Microbiology, 66(10): 4532–4535, doi: 10.1128/aem.66.10.4532-4535.2000

Pallud C, van Cappellen P. 2006. Kinetics of microbial sulfate reduction in estuarine sediments. Geochimica et Cosmochimica Acta, 70(5): 1148–1162, doi: 10.1016/j.gca.2005.11.002

Piza F F, Prado P I, Manfio G P. 2004. Investigation of bacterial diversity in Brazilian tropical estuarine sediments reveals high actinobacterial diversity. Antonie van Leeuwenhoek, 86(4): 317–328, doi: 10.1007/s10482-004-0162-5

Qin Wei, Heal K R, Ramdasi R, et al. 2017. *Nitrosopumilus maritimus* gen. nov., sp. nov., *Nitrosopumilus cobalaminigenes* sp. nov., *Nitrosopumilus oxyclinae* sp. nov., and *Nitrosopumilus ureiphilus* sp. nov., four marine ammonia-oxidizing archaea of the phylum Thaumarchaeota. International Journal of Systematic and Evolutionary Microbiology, 67(12): 5067–5079, doi: 10.1099/ijsem.0.002416

Schink B, Stieb M. 1983. Fermentative degradation of polyethylene glycol by a strictly anaerobic, gram-negative, nonsporeforming bacterium, *Pelobacter venetianus* sp. nov. Applied and Environmental Microbiology, 46(6): 1905–1913, doi: 10.1128/AEM.45.6.1905-1913.1983

Sia E S A, Zhu Zhuoyi, Zhang Jing, et al. 2019. Biogeographical distribution of microbial communities along the Rajang River–South China Sea continuum. Biogeosciences, 16(21): 4243–4260, doi: 10.5194/bg-16-4243-2019

Sintes E, Bergauer K, De Corte D, et al. 2013. Archaeal *amo*A gene diversity points to distinct biogeography of ammonia-oxidizing *Crenarchaeota* in the ocean. Environmental Microbiology, 15(5): 1647–1658, doi: 10.1111/j.1462-2920.2012.02801.x

Smith M W, Zeigler Allen L, Allen A E, et al. 2013. Contrasting genomic properties of free-living and particle-attached microbial assemblages within a coastal ecosystem. Frontiers in Microbiology, 4: 120, doi: 10.3389/fmicb.2013.00120

Sunagawa S, Coelho L P, Chaffron S, et al. 2015. Structure and function of the global ocean microbiome. Science, 348(6237): 1261359, doi: 10.1126/science.1261359

Wang Huan, Hu Zhangxi, Chai Zhaoyang, et al. 2020. Blooms of *Prorocentrum donghaiense* reduced the species diversity of dinoflagellate community. Acta Oceanologica Sinica, 39(4): 110–119, doi: 10.1007/s13131-020-1585-1

Wang Wentao, Yu Zhiming, Wu Zaixing, et al. 2018. Rates of nitrification and nitrate assimilation in the Changjiang River Estuary and adjacent waters based on the nitrogen isotope dilution method. Continental Shelf Research, 163: 35–43, doi: 10.1016/j.csr.2018.04.014

Wei Guangshan, Li Mingcong, Li Fenge, et al. 2016. Distinct distribution patterns of prokaryotes between sediment and water in the Yellow River Estuary. Applied Microbiology and Biotechnology, 100(22): 9683–9697, doi: 10.1007/s00253-016-7802-3

Wei Yongjun, Zhang Lei, Zhou Zhihua, et al. 2018. Diversity of gene clusters for polyketide and nonribosomal peptide biosynthesis revealed by metagenomic analysis of the Yellow Sea sediment. Frontiers in Microbiology, 9: 295, doi: 10.3389/fmicb.2018.00295

Wu Ying, Zhu Kun, Zhang Jing, et al. 2019. Distribution and degradation of terrestrial organic matter in the sediments of peat-draining rivers, Sarawak, Malaysian Borneo. Biogeosciences, 16(22): 4517–4533, doi: 10.5194/bg-16-4517-2019

Ye Qi, Wu Ying, Zhu Zhuoyi, et al. 2016. Bacterial diversity in the surface sediments of the hypoxic zone near the Changjiang Estuary and in the East China Sea. MicrobiologyOpen, 5(2): 323–339, doi: 10.1002/mbo3.330

Yu Y, Lee C, Kim J, et al. 2005. Group-specific primer and probe sets to detect methanogenic communities using quantitative real-time polymerase chain reaction. Biotechnology and Bioengineering, 89(6): 670–679, doi: 10.1002/bit.20347

Yu Yue, Wang Hui, Liu Jian, et al. 2012. Shifts in microbial community function and structure along the successional gradient of coastal wetlands in Yellow River Estuary. European Journal of Soil Biology, 49: 12–21, doi: 10.1016/j.ejsobi.2011.08.006

Zhang Jing, Du Ya'nan, Zhang Guosen, et al. 2021. Increases in the seaward river flux of nutrients driven by human migration and land-use changes in the tide-influenced delta. Science of the Total Environment, 761: 144501, doi: 10.1016/j.scitotenv.2020.144501

Zhang Xiaohui, Müller M, Jiang Shan, et al. 2020a. Distribution and flux of dissolved iron in the peatland-draining rivers and estuaries of Sarawak, Malaysian Borneo. Biogeosciences, 17(7): 1805–1819, doi: 10.5194/bg-17-1805-2020

Zhang Chunfang, You Shaohong, Dang Hongyue, et al. 2019. Redox characterization of humins in sediments from the Yangtze Estuary to the East China Sea and their effects on microbial redox reactions. Journal of Soils and Sediments, 19(5): 2594–2603, doi: 10.1007/s11368-018-02235-w

Zhang Zhaoru, Zhou Meng, Zhong Yisen, et al. 2020b. Spatial variations of phytoplankton biomass controlled by river plume dynamics over the lower Changjiang Estuary and adjacent shelf based on high-resolution observations. Frontiers in Marine Science, 7: 587539, doi: 10.3389/fmars.2020.587539

Zhu Q, van Prooijen B C, Wang Z B, et al. 2017. Bed-level changes on intertidal wetland in response to waves and tides: A case study from the Yangtze River Delta. Marine Geology, 385: 160–172, doi: 10.1016/j.margeo.2017.01.003

Supplementary information:

Fig. S1. Alpha diversity parameters of the 4 identified sample groups. a. Chao1 estimators; b. Dominance estimators; c. Equitability estimators; d. Richness estimators; e. Shannon_2 estimators; f. Simpson estimators.

Fig. S2. The results of ANOSIM show that the inter-group gap (e.g., MG1 vs. MG2) is greater than the intra-group difference.

Fig. S3. Abundance of sediment microbiota at the phylum-level (a) and genus-level (b) in the studied 48 sediment samples.

Fig. S4. Spatial distribution of temperature, salinity, turbidity and fluorescence of Chlorophyll a in bottom waters (2 m above seabed) in the continental shelf affected by the Changjiang River plume during March 2018 as measured with CTD vertical profiles. Dots represent CTD measurement sites.

Fig. S5. Spatial distribution of temperature, salinity, turbidity and fluorescence of Chlorophyll a in bottom waters in the continental shelf affected by the Changjiang River plume during July 2017. Dots represent CTD measurement sites.

Table S1. The obtained 16S rRNA fragment sequence and the alpha diversity parameters of the marine samples

Table S2. The top 20 most dominant OTUs, their distribution in each sample and the difference comparison between each group based on T-test analysis

The supplementary information is available online at https://doi.org/10.1007/s13131-021-1861-8 and http://www.aosocean.com/. The supplementary information is published as submitted, without typesetting or editing. The responsibility for scientific accuracy and content remains entirely with the authors.